Alternative Mechanisms for the Interaction of the Cell-Penetrating Peptides Penetratin and the TAT Peptide with Lipid Bilayers

Semen Yesylevskyy,[†¶] Siewert-Jan Marrink,[†] and Alan E. Mark[†‡§*]

[†]Groningen Biomolecular Sciences and Biotechnology Institute, Department of Biophysical Chemistry, University of Groningen, Groningen. The Netherlands; [‡]School of Chemistry and Molecular Biosciences and [§]Institute for Molecular Biosciences, University of Queensland, Brisbane, Australia; and [¶]Department of Physics of Biological Systems, Institute of Physics, National Academy of Sciences of Ukraine, Kiev, Ukraine

ABSTRACT Cell-penetrating peptides (CPPs) have recently attracted much interest due to their apparent ability to penetrate cell membranes in an energy-independent manner. Here molecular-dynamics simulation techniques were used to study the interaction of two CPPs: penetratin and the TAT peptide with 1,2-Dipalmitoyl-*sn*-glycero-3-phosphocholine (DPPC) and 1,2-dioleoyl-*sn*-glycero-3-phosphocholine (DOPC) phospolipid bilayers shed light on alternative mechanisms by which these peptides might cross biological membranes. In contrast to previous simulation studies of charged peptides interacting with lipid bilayers, no spontaneous formation of transmembrane pores was observed. Instead, the simulations suggest that the peptides may enter the cell by micropinocytosis, whereby the peptides induce curvature in the membrane, ultimately leading to the formation of small vesicles within the cell that encapsulate the peptides. Specifically, multiple peptides were observed to induce large deformations in the lipid bilayer that persisted throughout the timescale of the simulations (hundreds of nanoseconds). Pore formation could be induced in simulations in which an external potential was used to pull a single penetratin or TAT peptide into the membrane. With the use of umbrella-sampling techniques, the free energy of inserting a single penetratin peptide into a DPPC bilayer was estimated to be ~75 $kJmol^{-1}$, which suggests that the spontaneous penetration of single peptides would require a timescale of at least seconds to minutes. This work also illustrates the extent to which the results of such simulations can depend on the initial conditions, the extent of equilibration, the size of the system, and the conditions under which the simulations are performed. The implications of this with respect to the current systems and to simulations of membrane-peptide interactions in general are discussed.

INTRODUCTION

Cell membranes are effectively impermeable to hydrophilic compounds unless the permeation is facilitated by dedicated transport systems. This means that many hydrophilic compounds, including many promising drug candidates, fail to reach their intracellular target because they cannot spontaneously cross lipid membranes. As a consequence, there is much interest in finding ways to facilitate the transport of molecules across cell membranes. Cell-penetrating peptides (CPPs) in particular have shown much promise as potential delivery agents. CPPs are relatively short (<30 amino acids), positively charged peptides that have been claimed to penetrate cell membranes in an energy- and receptor-independent manner (1–3). In addition, CPPs lead to the internalization of various cargos to which they are attached. Although more than 100 CPPs have been identified, few have been studied in detail. Those for which experimental data are readily available include penetratin (4), the HIV-TAT peptide (5), transportan (6), MAP (7), and polyarginines of various lengths (8). CPPs in general have a net positive charge and are amphipathic; however, they do not have an obvious common sequence or structural motif. For example, unlike pore-forming peptides, such as melittin (9), the majority of CPPs do not possess well-defined hydrophilic or hydrophobic surfaces.

In this work, we focus on the mechanism of action of two naturally occurring CPPs: penetratin and the HIV TAT peptide. Penetratin, also called the pAntp peptide, is a part of the *Drosophila* Antennapedia homeodomain (amino acids 43–58, RQIKIWFQNRRMKWKK). In penetratin, 7 of the 16 residues are positively charged at neutral pH. The C-terminus of penetratin is usually amidated, as is common in other CPPs (1). The conformation of the penetratin peptide in the parent protein is helical. However, when isolated in solution, the peptide is largely unstructured (4), and alternative studies have suggested that the peptide is either partially α-helical (10) or has a partial β-hairpin structure (11). Indeed, it is possible that the actual structure in solution is concentration-dependent (12,13). The TAT peptide is part of the transcription transactivation (TAT) protein from human HIV-1 virus (residues 48–60, GRKKRRQRRRPPQ) (14,15). The TAT peptide contains seven positively charged residues. Again, the C-terminus is usually amidated (1). NMR studies suggest that the TAT peptide is unstructured in solution (16).

CPPs have attracted much interest because of their apparent ability to penetrate cells under conditions that prevent active energy-dependent transport, such as at low temperatures or in the presence of inhibitors of endocytosis (1,3). Although aspects of these studies have been questioned (17), a considerable body of evidence suggests that CPPs are not only able to bind to and insert within membranes, they can also

Submitted November 14, 2008, and accepted for publication March 30, 2009.

*Correspondence: a.e.mark@uq.edu.au

Editor: Alexandre M. J. J. Bonvin.

0006-3495/09/07/0040/10 $2.00

doi: 10.1016/j.bpj.2009.03.059

spontaneously penetrate cell membranes. A variety of possible mechanisms have been proposed that could give rise to the spontaneous penetration of membranes by these peptides. These include the carpet model (18), the formation of transient pores (19,20), the formation of inverted micelles (21), local electroporation (17), and direct insertion of the unfolded peptide into the membrane (22). A major difficulty in determining the actual mechanism by which CPPs act is that, experimentally, it is not possible to study the insertion of an individual peptide into a membrane with sufficient temporal and spatial resolution to distinguish between the various alternative models.

Although it is not possible to study the interaction between peptides and model membranes in atomic detail experimentally, theoretical approaches such as molecular-dynamics (MD) simulation techniques can provide detailed structural information on the time and length scales required. All-atom MD simulations of membrane-peptide systems are increasingly being used to address complex phenomena, including the spontaneous insertion of antimicrobial peptides into membranes (23–26).

Several simulation studies of membrane-CPP systems have been reported. Lensink et al. (27) simulated the behavior of penetratin in water and the spontaneous binding of a single penetratin peptide to neutral and charged lipid bilayers. In particular, they analyzed the role of different residues in binding and attempted to estimate the binding energy. Only one study has attempted to investigate the translocation process itself. Herce and Garcia (20) examined the interaction of TAT peptides with DOPC bilayers using various peptide concentrations and system sizes. The penetration of multiple peptides into the bilayer, leading to the spontaneous formation of a transmembrane pore on the timescale of 100–200 ns, was observed. The authors proposed that the mechanism of translocation of the TAT peptide involved the destabilization of the membrane by multiple peptides leading to the formation of a transmembrane pore through which individual peptides could diffuse, similar to what has been observed in simulations of antimicrobial peptides (23,26). Although this is an intriguing result, a number of questions remain. In particular, it is questionable whether the timescale on which the process was observed to occur is appropriate. Experimentally, the time required for the translocation of CPPs across a cell membrane is on the order of minutes (1,2). In contrast, atomistic MD simulations of membrane-peptide systems are restricted to hundreds of nanoseconds. As a consequence, the spontaneous translocation of CPPs is not expected to be observed in simulations that directly mimic experimental conditions.

In this work, the interaction of penetratin and the HIV-TAT peptide with 1,2-dipalmitoyl-*sn*-glycero-3-phosphocholine (DPPC) and 1,2-dioleoyl-*sn*-glycero-3-phosphocholine (DOPC) bilayers was investigated. Specifically, the spontaneous binding of single and multiple CPPs to different phospholipid bilayers was studied together with the effect of peptide aggregation on the integrity of the bilayer structure. In addition, the potential of mean force (PMF) associated with the translocation of a single peptide through the membrane was calculated.

No signs of spontaneous pore formation, as reported recently for the TAT peptide (20), were observed for either penetratin or the TAT peptide. Nevertheless, the penetratin and TAT peptides did induce dramatic changes in the structure of the membrane. The PMFs obtained from a combination of ''pulling'' and umbrella-sampling simulations suggest that there is a significant barrier to the penetration of both peptides into the membrane. In addition, it was found that the apparent effect of the peptides on the integrity of the membrane was strongly dependent on the size of the system studied and the nature of the simulation conditions used, and that even on a timescale of hundreds of nanoseconds the PMFs obtained were still sensitive to changes in the starting configuration. The implications of this for studies of peptide insertion into membranes in general are discussed further below.

MATERIALS AND METHODS

General setup

All simulations were performed using the GROMACS 3.3.1 suite of programs (28). The GROMOS 43a2 force field (29) was used to describe the peptide, and the lipids were described using the parameters of Berger et al. (30). Water molecules were described using the simple point charge water model (31). All simulations were performed under periodic boundary conditions at constant temperature and pressure. Unless otherwise stated, long-range electrostatic interactions were computed using the fourth-order particle mesh Ewald (PME) method (32) with a Fourier spacing of 0.15 nm. The real space coulombic interactions and the pair-list calculations were set to 1.0 nm. van der Waals interactions were computed using the shifted Lennard-Jones potential with a general cutoff of 1.1 nm and a shifting cutoff of 1.0 nm. Bond lengths within the peptides and lipids were constrained using the LINCS algorithm (33). The water molecules were constrained using SETTLE (34). A summary of the simulations performed and further details regarding the simulation protocol are provided in the Supporting Material (Table S1).

Peptides

The initial coordinates of penetratin were taken from the crystal structure of the Antennapedia homeodomain protein (PDB code 1AHD). The coordinates of missing atoms were obtained using the autopsf plug-in of the program VMD (35). The initial coordinates of the TAT peptide were taken from the NMR structure of the HIV-1 TAT protein (PDB code 1JFW, model 1). The C-termini of both peptides were amidated. Penetratin and the TAT peptide were first energy-minimized in vacuum and then placed in a truncated octahedral box and solvated by 2811 and 3692 water molecules, respectively. Since the peptides carry a net positive charge, Cl^- counterions were added to achieve neutrality of the system. Both systems were simulated for 25 ns under NPT conditions.

Pure bilayers

The topology of DPPC was the same as described previously (36). DOPC was constructed by modifying both alkyl chains of DPPC. Bilayers containing 128 lipids were constructed by arranging individual lipids on an 8×8 grid corresponding to each monolayer (64 lipids per monolayer). The systems

were placed in a rectangular box and solvated to obtain a water/lipid ratio of 38-40 corresponding to liquid crystalline DPPC at full hydration. The bilayers were equilibrated until the area per lipid stabilized (~50 ns). A bilayer containing 512 lipids (256 in each monolayer) was constructed by replicating the equilibrated 128-lipid system in the X and Y directions, where the Z axis is normal to the bilayer.

Peptide-bilayer systems

To construct the peptide-bilayer systems, one or more peptide molecules were oriented such that their principal axis was aligned with the X axis of the box, and placed above the bilayer so that the minimum distance between any heavy atom of peptide and the bilayer was 0.2 nm. Water molecules that overlapped with the peptides were removed, Cl^- counterions were added to neutralize the system, and each system was energy-minimized before the simulations were initiated.

Pulling

To study the process of penetration, which is slow compared to the timescale of the simulations (~100 ns), an external force was applied to the peptide to accelerate the rate at which it entered the membrane. A harmonic potential with a force constant of 1000 kJ/mol/nm^2 was applied between the center of mass of the peptide and a reference position along the Z axis determined with respect to the center of mass of the membrane. The reference position was then moved at a rate of 10^{-4} nm/ns. The motion of the peptide in the XY plane was not restrained. Reference values of $Z > 0$ nm and $Z < 0$ nm correspond to the ''upper'' and ''lower'' monolayers, respectively. Two pulling simulations were performed for each system. The first involved the gradual change in the reference position from $Z = 3.2$ nm (i.e., above the upper monolayer) to $Z = -3.0$ nm (i.e., below the lower monolayer), causing the peptide to be dragged through the middle of the bilayer. The second pulling experiment was performed in the opposite direction from $Z = -1.0$ nm (i.e., the hydrophobic part of the ''lower'' monolayer) to $Z = 1.5$ nm (i.e., the center of the ''upper'' monolayer).

Umbrella sampling

To determine the free-energy profile of translocation, umbrella sampling (37) techniques were used. Snapshots from the pulling trajectories were used to initiate a series of simulations in which the center of mass of the peptide was harmonically restrained as described above at a series of fixed Z values. Configurations from the forward trajectory were selected every 0.05 nm in the range $Z = \sim 3.2$ nm (i.e., above the upper monolayer in the bulk water) to $Z = 0$ nm (i.e., the center of the bilayer), and from the reverse trajectory in the range $Z = -1.0$ nm to $Z = \sim 1.5$ nm, again at 0.05 nm intervals, resulting in 51–71 windows depending on the system. Each window was simulated for up to 100 ns and the free-energy profiles were constructed using the umbrella integration technique (37) (see Supporting Material).

RESULTS

Peptides in water

Consistent with the results of previous MD studies (27), penetratin, which was initially placed in a fully α-helical conformation, was found to partially unfold, with only the central portion of the peptide (residues 47–55) remaining helical (Fig. S1). Although the time simulated (25 ns) is clearly too short to sample a true equilibrium distribution of states, previous studies (27) suggest that such a partially helical state is stable for hundreds of nanoseconds. Therefore, the structure at 25 ns was used as the starting conformation for all subsequent simulations. In contrast to penetratin, which remained partly helical, the TAT peptide sampled a wide range of conformations during the 25 ns of simulation (Fig. S1). This is in line with available NMR data suggesting that the peptide is unstructured in solution (16). Again, the final conformation after 25 ns of simulation was used as the starting structure in all subsequent work.

Spontaneous binding and aggregation

Possible alternative mechanisms by which CPPs could act include the direct disruption of the membrane and/or the formation of a transmembrane pore (20). To study the spontaneous binding of the peptides to a lipid bilayer, as well as the potential for the peptides to induce the formation of pores, a series of MD simulations of different peptide membrane systems was performed.

First, a system similar to that simulated by Herce and Garcia (20) was investigated. Starting from an equilibrated DOPC bilayer containing 128 lipids, a series of four TAT peptides were added consecutively close to one side of the bilayer. The system was equilibrated for 10 ns after the addition of each peptide. To ensure that all peptides bound to the same monolayer, a weak harmonic potential (force constant 30 kJ/mol/nm^2) was applied between the center of mass of each peptide and the center of the bilayer (Z direction only). When all four peptides were bound to the membrane, the biasing potential was removed and the system was simulated for 200 ns without restraints. Two systems were simulated: one in which counterions were included to ensure the electroneutrality of the system, and one without counterions, replicating the setup used by Herce and Garcia (20). In both cases, the long-range electrostatic interactions were calculated using the PME approach. No signs of spontaneous pore formation were observed within 200 ns with or without counterions. The peptides appeared to diffuse randomly on the surface of the membrane and showed little tendency to either aggregate or penetrate into the membrane. The membrane itself remained planar. The primary difference between the simulations with and without counterions was in the area per lipid. The area per lipid in the system with counterions was 0.64 nm^2, close to that obtained for pure DOPC (38,39). In contrast, the area per lipid for the system without counterions was 0.79 nm^2, close to the value reported by Herce and Garcia (20). The bilayer had thinned significantly, suggesting it was under considerable stress (see Fig. S2).

Binding of multiple peptides to large bilayer patches

A bilayer patch of just 128 lipids is heavily constrained by the imposition of periodic boundary conditions. For this reason, the effect of the addition of peptides to a DPPC bilayer patch consisting of 512 lipids was investigated. Eight penetratin and eight TAT peptides were added to separate systems. Again, a weak harmonic potential (force constant

30 kJ/mol/nm^2) was applied between the center of mass of each peptide and the center of the bilayer along the Z axis to ensure that all peptides bound to the same side of the membrane. The biasing potential was removed after the peptides bound to the membrane and each system was simulated for ~50 ns.

For the first 10 ns the peptides appeared to diffuse randomly on the surface of the membrane, forming dimers but causing little obvious disruption of the membrane (Fig. 1 *a*). As larger aggregates formed, the membrane began to deform (Fig. 1 *b*). The peptides migrated toward the center of the depression, forming a compact cluster (Fig. 1 *c*). This continued until the membrane began to encapsulate the cluster of peptides (Fig. 1 *d*). To ensure that the distortion of the membrane was not due to periodicity artifacts induced by the use of the PME approach, the calculations were repeated using a cutoff together with a long-range correction based on a generalized reaction field approach with a dielectric constant of 80 (40). The results obtained using the two alternative approaches were essentially identical.

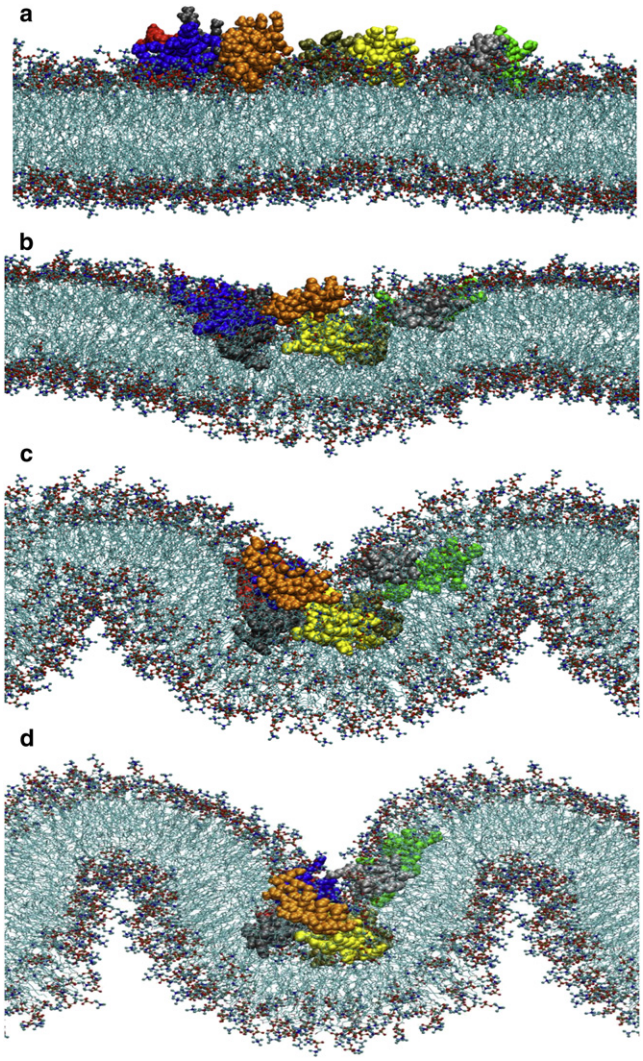

FIGURE 1 Stages of the deformation of a DPPC bilayer with 512 lipids and eight bound penetratin peptides. The lipid tails are shown as sticks, lipid headgroups are shown as balls and sticks, and the peptides are in space-filling representation. Each peptide is shown in a different color. See text for details. The unit cell is replicated in the X direction to make the buckled shape of the membrane clearly visible. For clarity, water molecules are not shown.

Pulling simulations

Because it was not possible to observe the spontaneous penetration of either penetratin or the TAT peptide on the timescale of the simulations, a harmonic restraining potential was applied between the center of mass of a single peptide and a reference point fixed relative to the center of the membrane, which was then moved at a rate of 10^{-4} nm ns^{-1} in the direction normal to the plane of the membrane. This caused the peptide to move across the bilayer, as illustrated in Fig. 2 for the case of penetratin interacting with a DPPC bilayer. Placed initially above the plane of the membrane (Fig. 2 *a*), the peptide bound parallel to the plane of the membrane, resulting in a slight depression within the upper monolayer. The structure of the lower monolayer was unaffected (Fig. 2 *b*). As the restraining potential acting on peptide was increased with time, the center of mass of peptide moved toward the center of the bilayer (Fig. 2 *c*). The distortion within the upper monolayer gradually increased until a critical point was reached, at which time the formation of a hydrophilic toroidal-like pore was observed (Fig. 2 *d*). The surface of the pore was lined with lipid headgroups and the pore itself was filled with water. Once formed, the pore was stable and remained largely unchanged until the center of mass of the peptide reached the lipid-water interface of the lower monolayer (Fig. 2 *e*). After the center of mass of the peptide was pulled beyond the plane of the lower monolayer, the membrane again began to deform due to interactions between the peptide and the membrane (Fig. 2 *f*). Finally, the interactions with the membrane rupture, with several lipids remaining bound to the peptide. If the direction of pulling was reversed before the interactions between the membrane and the peptide were disrupted, the peptide simply moved back through the pore. Distortions in the membrane were again observed, however, as the peptide was dragged beyond the upper monolayer. Equivalent results were obtained in the case of the TAT peptide (results not shown).

Umbrella sampling

The pulling experiments described above are clearly far from equilibrium. In an attempt to generate an equilibrium free-energy profile for the translocation of penetratin and the TAT peptide across a DPPC bilayer, configurations extracted from the pulling trajectories were used as starting points for a series of umbrella sampling simulations. In these simulations the center of mass of the peptide was restrained to a particular depth within the membrane, separated by 0.01 nm intervals, and the systems were monitored for up to 180 ns.

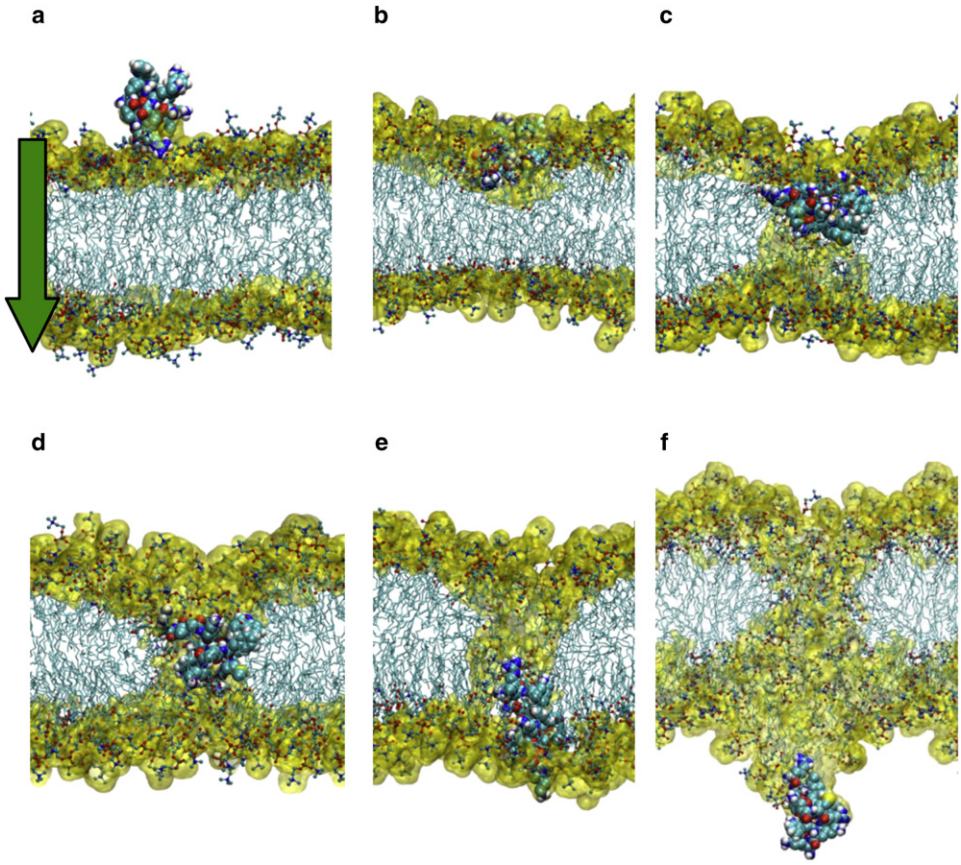

FIGURE 2 Key stages during the pulling of a single penetratin molecule through a DPPC bilayer. The peptide is shown in space-filling representation, and the lipid headgroups are shown in a ball and stick representation. The lipid tails are shown as sticks. The semitransparent yellow surface corresponds to the lipid-water interface. The arrow indicates the direction in which the pulling force is applied. (*a*) The initial system. (*b*) The peptide binds to the upper monolayer. (*c*) The water-filled pore is formed. (*d*) The peptide reaches the center of bilayer. (*e*) The peptide reaches the surface of the lower monolayer. (*f*) The peptide is pulled out of the membrane (the state before complete membrane disruption). Panel *f* is shown in a slightly reduced scale.

The free-energy profiles or PMFs, estimated using the umbrella integration technique (37) (see Materials and Methods) for successive 20 ns windows, are shown in Fig. 3. The PMF is plotted from just before the center of the membrane ($Z = -0.3$ nm) to where the peptide is surrounded by bulk solvent and no longer interacts directly with the bilayer ($Z = 3.5$ nm). The overall shape of the PMF is very similar for both peptides. There is a maximum in the PMF close to the center of the bilayer ($Z = 0$ nm) and a shallow minimum ($Z = 2.0$–2.5 nm) corresponding to where the peptide is interacting with the bilayer-water interface. As is evident from Fig. 3, the height of the maximum decreases with increasing equilibration time. In addition, although the PMF is expected to be symmetric with respect to the center of bilayer ($Z = 0$), on close inspection it can be seen that it is not. This shows that although the system was allowed to equilibrate for at least 80 ns in each window, the PMFs have still not fully converged. Nevertheless, two important features regarding Fig. 3 should be noted. First, there is a marked kink in the PMFs around 0.5–0.6 nm, which becomes more pronounced as the system is equilibrated. This kink, which is indicated by the arrows in Fig. 3, marks

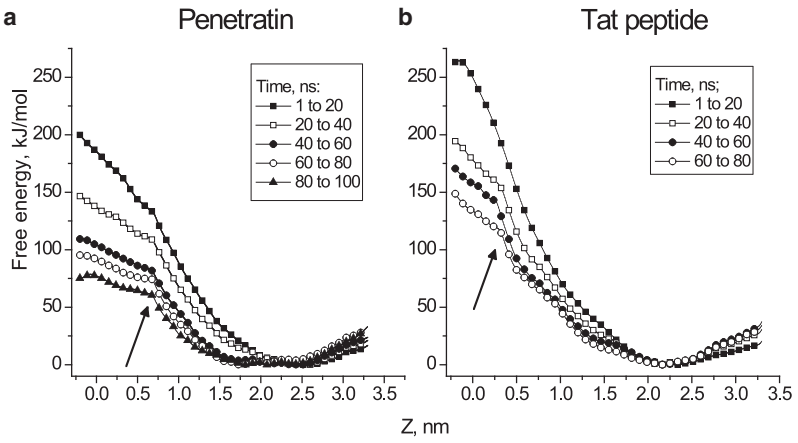

FIGURE 3 The free-energy profile (or PMF) for the translocation of (*a*) penetratin and (*b*) the TAT peptide through a DPPC bilayer computed using the umbrella integration technique (37). The different curves correspond to averages over different simulation times. $Z = 0$ nm corresponds to the center of the membrane. The arrow indicates the position at which a pore is formed.

the separation between when the peptide lies within the central region of the membrane, and the barrier associated with the peptide crossing the interfacial region. Visual inspection of the trajectories shows that the kink is associated with the formation of the transmembrane pore. The second notable feature is that the free-energy barrier to translocation is consistently lower in the case of penetratin than for the TAT peptide.

To examine the sensitivity of the PMFs obtained to the initial configurations used in each window, the calculations were repeated using configurations taken from the simulations in which the direction of pulling was reversed, i.e., starting from $Z = -1.0$ nm and continuing until $Z = 1.5$ nm. Note that the direction in which the peptide was pulled was reversed after a transmembrane pore formed. The calculations were performed only for the case of the penetratin-DPPC system. The results using configurations from the forward and reverse pulling trajectories for different sampling times are shown in Fig. 4. In regard to Fig. 4, it should be noted that although the simulations at each value of Z are in principle independent, the umbrella integration technique uses a weighting procedure that combines the results from a range of windows to obtain the force at a specific value of Z. It is this value that is then used to generate the PMF profiles shown in Figs. 3 *a* and 5. This procedure in effect smoothes the force profile and explains why the variation in the forces at adjacent values of Z for different sampling times appear correlated in Fig. 4.

The first thing that can be noted from Fig. 4 is that the overall shape of the curves corresponding to configurations taken from the forward (*black curves*) and reverse (*gray curves*) pulling trajectories differ significantly even after extensive equilibration (*squares* and *circles* in Fig. 4). The forces are similar in the central region of the membrane (near $Z = 0$ nm), suggesting that the values in this region are nearly converged, but diverge significantly after $Z = 0.1$ nm. Specifically, in the region between the center of the membrane and the point where the pore is first formed (from $Z = 0.1$ nm to $Z = 0.6$ nm), the mean force is positive in the case of the forward pulling configurations, indicating that work is required to pull the peptide *toward* the center of the membrane. However, it is negative in the case of the reverse pulling configurations, indicating that work is required to pull the peptide *away* from the center of the membrane. Furthermore, a sharp discontinuity at $Z \approx 0.6$ nm is evident in the forward pulling configurations, but not in the reverse pulling configurations. To determine whether it is possible to obtain convergence in the center of the membrane, nine windows located in the range $Z = 0.1$–0.5 nm from the forward and reverse pulling trajectories were each simulated for an additional 50 ns starting from 80 ns in the case of forward pulling configurations, and from 20 ns in the case of reverse pulling configurations. As can be seen from Fig. 4 *b* (*triangles*), extending the trajectories resulted in the forces from both the forward and reverse pulling configurations converging to similar values.

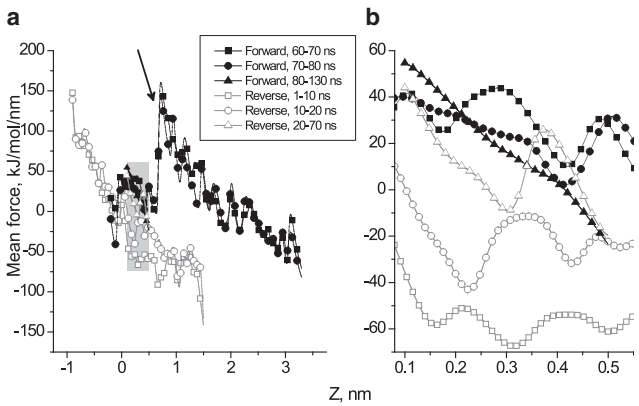

FIGURE 4 The mean force as obtained using the umbrella integration technique for the translocation of penetratin through a DPPC bilayer using structures taken from the forward and reverse pulling simulations for different averaging times. The region from $Z = 0.1$ to $Z = 0.5$ (*shaded* in *a*) is enlarged in *b*. $Z = 0$ nm corresponds to the center of the membrane. The discontinuity indicated by the arrow corresponds to the onset of pore formation in the case of the configurations from forward pulling trajectories.

DISCUSSION

Although MD simulations of membrane systems have progressed dramatically in recent years, and phenomena such as pore formation by simple antimicrobial peptides (23,26) have been simulated in atomic detail, simulating the translocation of CPPs through a membrane represents a major increase in complexity over previous studies. In particular, the spontaneous translocation of the peptide across a membrane is known from experiment to be a rare process, with rates on the order of single events per minute (1). Spontaneous translocation events are not expected to be observed on the timescales accessible to MD simulations performed under experimental-like conditions, unless nonphysical restraints are applied to accelerate the underlying process.

Experimentally, it is not known whether penetratin or the TAT peptide aggregates before penetrating the membrane. Although some studies (41,42) suggest the TAT peptide forms clusters on the surface of membranes, it is not known whether such clusters are required for translocation. Previous simulation studies suggested that although single copies of penetratin or the TAT peptide readily bind to the surface of lipid bilayers, they do not penetrate on timescales of up to 200 ns (20,27). This is in line with an increasing body of work involving both experiments and simulations that suggests that many pore-forming antimicrobial peptides are active only as aggregates (23,41–43).

Spontaneous pore formation

Herce and Garcia (20) recently reported the spontaneous formation of hydrophilic pores in simulations of multiple copies of the TAT peptide bound to a DOPC bilayer. This work is important in that it provided a possible model for the process of translocation. However, the fact that the

formation of the pore occurred spontaneously within 200 ns raises serious questions as to whether the simulations represent the experimental system appropriately. In particular, pore formation in the simulations of Herce and Garcia was only observed at very high ratios of peptide to lipid (P/L = 1:18) or at elevated temperature, and without the inclusion of counterions. Since each of the TAT peptides carried a net charge of +7, this meant that the system overall was strongly charged, leading to possible artifacts. In fact, in the simulations of Herce and Garcia (20), the bilayer area/lipid expanded to ~0.8 nm^2. The lateral expansion of the bilayer and the associated thinning of the hydrophobic core may explain why the spontaneous formation of pores was observed in these simulations. Of particular note is the fact that Herce and Garcia used PME to calculate the long-range electrostatic interactions. In this case, instead of counterions being used to neutralize the system, a uniform background charge is added to the system to ensure overall electroneutrality (44), which may account for the expanded area per lipid. To test this possibility, simulations were performed of multiple copies of the TAT peptide interacting with a DOPC bilayer (P/L = 1:32) in which counterions were added to the system to achieve overall neutrality. In these simulations no thinning was observed, and the area per lipid varied between 0.65 and 0.68 nm^2, close to the range (0.63–0.7 nm^2) of area per lipid reported for pure DOPC (38). This suggests that the use of PME without counterions in this system can lead to severe distortions in the bilayer due to the introduction of the uniform background charge induced by the peptide, as opposed to the peptide itself. Simulations were also performed under conditions equivalent to those of Herce and Garcia (20) (i.e., using PME and no counterions). In these simulations an area per lipid similar to that reported by Herce and Garcia (20) (0.78–0.8 nm^2) was obtained; however, no signs of spontaneous pore formation or deformation of the membrane were observed. Note that Herce and Garcia did not observe spontaneous pore formation at ambient temperatures for P/L ratios smaller than 1:18.

Micropinocytosis

The type of deformation that can be observed in simulations of small membrane patches consisting of only 128 lipids is limited by the periodic boundary conditions. Although simple deformations, such as the formation of a pore leading to membrane rupture, are possible, larger deformations, such as bending or invagination of the membrane, are not. When eight copies of Penetrin or the TAT peptide were bound to a DPPC membrane consisting of 512 lipids, the membrane was observed to wrap around the cluster of peptides, forming a deep groove (Fig. 1 *d*). To our knowledge, such large-scale deformations due to the presence of peptides have not been previously reported in simulations of membrane systems. Of importance, the process illustrated in Fig. 1 *d* would be the initial step in an alternative mechanism, known as micropinocytosis, by which CPPs could enter cells. Micropinocytosis does not require the formation of a transmembrane pore. Instead, the invagination caused by the membrane wrapping around the cluster of peptides would become detached from the membrane, leading to the formation of a spherical or tubular vesicle within the cell that encapsulated the peptides. Such a micropinocytosis mechanism was previously suggested to be involved in the internalization of certain CPPs (45,46). Alternatively, the invaginations could simply rupture, releasing the peptides into the cytosole. An interesting aspect of this mechanism is that it depends primarily on there being a high charge density on the surface of the membrane, such as is induced by the aggregation of the peptides. For example, a similar phenomenon has been observed in simulations of large patches of lipid bilayers containing an asymmetric distribution of charged lipids between the monolayers or domains of charged lipids (A.H. de Vries, University of Groningen, personal communication, 2008). This might explain how penetratin, the TAT peptide, and other charged CCPs could act via a similar mechanism despite having very different physicochemical and structural properties.

Translocation of a single peptide and PMF calculations

Micropinocytosis and pore formation by multiple peptides are two possible mechanisms that might explain the energy-independent translocation of CPPs; however, both require the presence of very high, and potentially nonphysical, local concentrations of peptide. To investigate how a single peptide might cross a membrane, a series of pulling simulations were performed in which a single penetratin or TAT peptide was forced to cross a DPPC membrane. These simulations showed that even a single peptide could induce the formation of a transmembrane pore and thus could in principle transport cargo molecules. To determine whether this mechanism is possible from a thermodynamic perspective, the free-energy profile (also known as the PMF) for the translocation of both peptides across a DPPC bilayer was computed. To obtain the correct PMF, the system must sample an equilibrium distribution of states within each window. Although ensuring that an equilibrium distribution has been sampled is relatively straightforward in the case of the translocation of a small molecule or ion, it represents a major challenge in cases involving large, flexible molecules such as CPPs. In particular, since the rotational diffusion of peptides in the membrane is slow on the timescale of the simulations, great care must be taken in generating the initial conformations. Here, snapshots from the pulling simulations were used as starting structures for the umbrella sampling simulations. This approach ensured that the starting structures for different windows were generated in a consistent manner. However, it also means the configurations in the successive windows were correlated. The fact that the peptide induces the formation of a transmembrane pore as it is dragged into the center

of the bilayer presents another complication in obtaining a converged PMF. Once formed, such transmembrane pores can be stable for many tens, if not hundreds, of nanoseconds. This led to a pronounced hysteresis between pulling simulations in the forward and reverse directions, which made it difficult to sample a true equilibrium distribution on the timescales accessible. This was true for both the formation of the pore and the release of the peptide from the membrane.

In principle, to obtain a converged PMF in such cases it is necessary to sample configurations in which a pore is present, and states that do not contain a pore. That is, the length of sampling must be much longer than the time required for pore formation and collapse at all values of Z. The extent of sampling that would be required to obtain a fully converged profile is most evident if one compares the forces acting on the penetratin peptide in simulations using configurations taken from the forward and reverse pulling trajectories (Fig. 4). Whereas the forces are similar in the central region of the membrane near $Z = 0$ nm (suggesting convergence), they diverge and even have opposite signs in the region $Z = 0.5$–1.5 nm. In particular, there is a sharp discontinuity at $Z \approx 0.6$ nm in the case of the forward pulling configurations, but not in the case of the reverse pulling configurations. This discontinuity corresponds to the kink in the PMF (Fig. 3) associated with the formation of the pore and the reorientation of the peptide. Although the peptide always lies along the water-membrane interface, it rotates from being parallel to the plane of the bilayer (without a pore) to more perpendicular to the plane of the bilayer (with a pore). Note that in both cases the conformation of the peptide, although fluctuating, remains similar to that in solution (the TAT peptide is largely unstructured, whereas penetratin retains some helical content). A similar kink is not observed starting from the reverse pulling configurations as the pore is meta-stable on the timescale of the simulations, and persists even after the peptide is dragged beyond the bilayer-water interface.

The time required for the formation and collapse of the pores is clearly long compared with the timescale simulated. This, together with the fact that the peptides sample a range of conformations and orientations, leads to significant hysteresis in the profiles. Because of these difficulties, only isolated peptides were considered in the pulling simulations. One way to improve sampling in such systems might be to use coarse-grained models (47) in which chemical detail is sacrificed to enhance speed. However, in cases such as this, which involves changes in conformation, the burial of charged residues, and induction of pores, and for which specific interactions are likely to be critical, such coarse-grained approaches would in general be less appropriate.

Fig. 5 shows the best estimate of the PMF for penetratin. This free-energy profile was obtained by combining the results from the extended simulations in the region $Z =$ 0–0.5 nm and using the results from the forward pulling trajectory from 80 to 100 ns for the region $Z = 0.5$–3.5 nm. The complete profile was obtained by reflecting the PMF

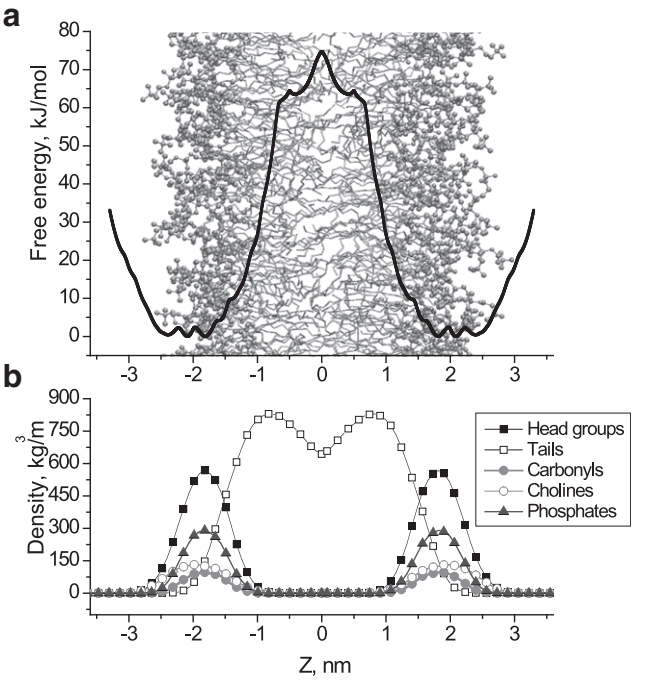

FIGURE 5 (*a*) The best estimate free-energy profile (PMF) for the translocation of penetratin through a DPPC bilayer obtained by combining results shown in Figs. 3 *a* and 4 superimposed on the structure of pure DPPC bilayer. Headgroups are shown as balls and sticks, and the lipid tails are shown as lines. The PMF is obtained by mirroring the right half around $Z = 0$ nm. (*b*) The density distributions of various lipid groups, which correspond to the bilayer in *a*.

about $Z = 0$ nm. The overall umbrella sampling calculations suggest that 1), the rate-limiting step for the translocation of a single peptide would be the formation of a transmembrane pore; 2), the height of the barrier associated with a single peptide entering the membrane and forming a pore is consistently greater in the case of the TAT peptide compared to penetratin within a specific simulation time, suggesting that penetratin should translocate more readily than the TAT peptide; and 3), even a single peptide can stabilize a transmembrane pore, and once the pore is formed, the diffusion of the peptide across the membrane within that pore is expected to be rapid. Note that the height of the barrier to the translocation of a single penetratin molecule is predicted to be $\leq$75 kJ/mole. Of interest, the height of the barrier is similar to that found for the translocation of lipids, which is also pore-mediated (48). Although these barriers are high, a simple application of Eyring theory suggests that barriers of this magnitude are in principle accessible at 300 K on timescales as low as seconds to minutes depending on the effective prefactor. The barriers to the translocation of primarily hydrophobic peptides appear to be significantly lower. For example, Babakhani et al. (49) determined the PMF for the translocation of model hexapeptide WL5 and found no pore formation, with the PMF showing a minimum of ~45 kJ/mol in the hydrophobic region of the membrane.

CONCLUSIONS

In this work, MD simulation techniques were used to investigate the mechanism by which the CPPs penetratin and the TAT peptide interact with membranes. In contrast to previous simulation studies, no spontaneous formation of transmembrane pores was observed on the timescales investigated. Instead, the simulations suggest that micropinocytosis may explain how CPPs facilitate the transport of cargo molecules into cells. Although pore formation induced by either a single peptide or a cluster of peptides remains a possible mechanism by which CPPs act, this work highlights the fact that one must use extreme caution when interpreting simulations, especially when specific events occur on unrealistic timescales. More generally, it shows that only when large bilayer patches ($\geq$500 lipids) are used can alternative mechanisms that involve large-scale deformation of the membrane, such as micropinocytosis, be tested. Furthermore, even when sampling times exceeding a total of 20 μs (100 ns per window) were used, it was still not possible to obtain fully converged profiles for the free energy associated with inserting a peptide into a membrane.

SUPPORTING MATERIAL

One table and two figures are available at http://www.biophysj.org/biophysj/supplemental/S0006-3495(09)00846-7.

This work was supported by a Marie Curie International Incoming Fellowship to S.Y. (MIF1-CT-2006-039150). S.Y. acknowledges the Netherlands Organisation for Scientific Research for allowing access to the Netherlands national computer facility SARA (grant MP-143). A.E.M. is an Australian Research Council Federation Fellow.

REFERENCES

1. Zorko, M., and U. Langel. 2005. Cell-penetrating peptides: mechanism and kinetics of cargo delivery. *Adv. Drug Deliv. Rev.* 57:529–545.
2. Deshayes, S., M. C. Morris, G. Divita, and F. Heitz. 2005. Cell-penetrating peptides: tools for intracellular delivery of therapeutics. *Cell. Mol. Life Sci.* 62:1839–1849, (CMLS).
3. Lindgren, M., M. Hallbrink, A. Prochiantz, and U. Langel. 2000. Cell-penetrating peptides. *Trends Pharmacol. Sci.* 21:99–103.
4. Derossi, D., A. H. Joliot, G. Chassaing, and A. Prochiantz. 1994. The third helix of the Antennapedia homeodomain translocates through biological membranes. *J. Biol. Chem.* 269:10444–10450.
5. Fawell, S., J. Seery, Y. Daikh, C. Moore, L. L. Chen, et al. 1994. Tat-mediated delivery of heterologous proteins into cells. *Proc. Natl. Acad. Sci. USA.* 91:664–668.
6. Pooga, M., M. Hallbrink, M. Zorko, and Ü. Langel. 1998. Cell penetration by transportan. *FASEB J.* 15:1451–1453.
7. Oehlke, J., A. Scheller, B. Wiesner, E. Krause, M. Beyermann, et al. 1998. Cellular uptake of an α-helical amphipathic model peptide with the potential to deliver polar compounds into the cell interior non-endocytically. *Biochim. Biophys. Acta.* 1414:127–139.
8. Wender, P. A., D. J. Mitchell, K. Pattabiraman, E. T. Pelkey, L. Steinman, et al. 2000. The design, synthesis and evaluation of molecules that enable or enhance cellular uptake: peptoid molecular transporters. *Proc. Natl. Acad. Sci. USA.* 97:13003–13008.
9. Hristova, K., C. E. Dempsey, and S. H. White. 2001. Structure, location, and lipid perturbations of melittin at the membrane interface. *Biophys. J.* 80:801–811.
10. Salamon, Z., G. Lindblom, and G. Tollin. 2003. Plasmonwaveguide resonance and impedance spectroscopy studies of the interaction between penetratin and supported bilayer membranes. *Biophys. J.* 84:1796–1807.
11. Bellet-Amalric, E., D. Blaudez, B. Desbat, F. Graner, F. Gauthier, et al. 2000. Interaction of the third helix of Antennapedia homeodomain and a phospholipid monolayer, studied by ellipsometry and PM-IRRAS at the air-water interface. *Biochim. Biophys. Acta.* 1467:131–143.
12. Magzoub, M., L. E. Eriksson, and A. Graslund. 2002. Conformational states of the cell-penetrating peptide penetratin when interacting with phospholipid vesicles: effects of surface charge and peptide concentration. *Biochim. Biophys. Acta.* 1563:53–63.
13. Magzoub, M., K. Kilk, L. E. Eriksson, U. Langel, and A. Graslund. 2001. Interaction and structure induction of cell-penetrating peptides in the presence of phospholipid vesicles. *Biochim. Biophys. Acta.* 1512:77–89.
14. Frankel, A. D., and C. O. Pabo. 1988. Cellular uptake of the tat protein from human immunodeficiency virus. *Cell.* 55:1189–1193.
15. Astriab-Fisher, A., D. Sergueev, M. Fisher, B. R. Shaw, and R. L. Juliano. 2002. Conjugates of antisense oligonucleotides with the Tat and Antennapedia cell-penetrating peptides: effects on cellular uptake, binding to target sequences and biologic actions. *Pharm. Res.* 19:744–754.
16. Peloponese, J.-M., C. Gregoire, S. Opi, D. Esquieu, J. Sturgis, et al. 2000. 1H–13C nuclear magnetic resonance assignment and structural characterization of HIV-1 Tat protein. *C.R. Acad. Sci. III.* 323:883–894.
17. Drin, G., S. Cottin, E. Blanc, A. R. Rees, and J. Temsamani. 2003. Studies on the internalization mechanism of cationic cell-penetrating peptides. *J. Biol. Chem.* 278:31192–31201.
18. Taylor, C. T., G. T. Furuta, K. Synnestvedt, and S. P. Colgan. 2000. Phosphorylation-dependent targeting of cAMP response element binding protein to the ubiquitin/proteasome pathway in hypoxia. *Proc. Natl. Acad. Sci. USA.* 97:12091–12096.
19. Gazit, E., W. J. Lee, P. T. Brey, and Y. Shai. 1994. Mode of action of the antibacterial cecropin B2: a spectrofluorometric study. *Biochemistry.* 33:10681–10692.
20. Herce, H. D., and A. E. Garcia. 2007. Molecular dynamics simulations suggest a mechanism for translocation of the HIV-1 TAT peptide across lipid membranes. *Proc. Natl. Acad. Sci. USA.* 104:20805–20810.
21. Derossi, D., S. Calvet, A. Trembleau, A. Brunissen, G. Chassaing, et al. 1996. Cell internalization of the third helix of the Antennapedia homeodomain is receptor independent. *J. Biol. Chem.* 271:18188–18193.
22. Schwarze, S. R., K. A. Hruska, and S. F. Dowdy. 2000. Protein transduction: unrestricted delivery into cells? *Trends Cell Biol.* 10:290–295.
23. Leontiadou, H., A. E. Mark, and S. J. Marrink. 2006. Antimicrobial peptides in action. *J. Am. Chem. Soc.* 128:12156–12161.
24. Marrink, S. J., A. H. de Vries, and D. P. Tieleman. 2009. Lipids on the move: simulations of membrane pores, domains, stalks and curves. *Biochim. Biophys. Acta.* 1788:149–168.
25. Mátyus, E., C. Kandt, and D. P. Tieleman. 2007. Computer simulation of antimicrobial peptides. *Curr. Med. Chem.* 14:2789–2798.
26. Sengupta, D., H. Leontiadou, A. E. Mark, and S. J. Marrink. 2008. Toroidal pores formed by antimicrobial peptides show significant disorder. *Biochim. Biophys. Acta.* 1778:2308–2317.
27. Lensink, M. F., B. Christiaens, J. Vandekerckhove, A. Prochiantz, and M. Rosseneu. 2005. Penetratin-membrane association: W48/R52/W56 shield the peptide from the aqueous phase. *Biophys. J.* 88:939–952.
28. van der Spoel, D., E. Lindahl, B. Hess, G. Groenhof, A. E. Mark, et al. 2005. GROMACS: fast, flexible and free. *J. Comput. Chem.* 26:1701–1718.
29. van Gunsteren, W. F., P. Krüger, S. R. Billeter, A. E. Mark, A. A. Eising, et al. 1996. Biomolecular Simulation: The GROMOS96 Manual and User Guide. Biomos/Hochschulverlag AG an der ETH Zürich, Groningen/Zürich.

30. Berger, O., O. Edholm, and F. Jahnig. 1997. Molecular dynamics simulations of a fluid bilayer of dipalmitoylphosphatidylcholine at full hydration, constant pressure, and constant temperature. *Biophys. J.* 72:2002–2013.

31. Berendsen, H. J. C., J. P. M. Postma, W. F. van Gunsteren, and J. Hermans. 1981. Interaction models for water in relation to protein hydration. *In* Intermolecular Forces. B. Pullman, editor. Reidel, Dordrecht, The Netherlands. 331–342.

32. Tom, D., Y. Darrin, and P. Lee. 1993. Particle mesh Ewald: an N [center-dot] log(N) method for Ewald sums in large systems. *J. Chem. Phys.* 98:10089–10092.

33. Hess, B., H. Bekker, H. J. C. Berendsen, and J. G. E. M. Fraaije. 1997. LINCS: a linear constraint solver for molecular simulations. *J. Comput. Chem.* 18:1463–1472.

34. Miyamoto, S., and P. A. Kollman. 1992. SETTLE: an analytical version of the SHAKE and RATTLE algorithm for rigid water models. *J. Comput. Chem.* 13:952–962.

35. Humphrey, W., A. Dalke, and K. Schulten. 1996. VMD—visual molecular dynamics. *J. Mol. Graph.* 14:33–38.

36. Anezo, C., A. H. deVries, H. D. Holtje, D. P. Tieleman, and S. J. Marrink. 2003. Methodological issues in lipid bilayer simulations. *J. Phys. Chem. B.* 107:9424–9433.

37. Kästner, J., and W. Thiel. 2005. Bridging the gap between thermodynamic integration and umbrella sampling provides a novel analysis method: ''umbrella integration''. *J. Chem. Phys.* 123:144104.

38. Wiener, M. C., and S. H. White. 1992. Structure of fluid DOPC determined by joint refinement of X-ray and neutron diffraction data. III. Complete structure. *Biophys. J.* 61:434–447.

39. Tristram-Nagle, S., H. I. Petrache, and J. F. Nagle. 1998. Structure and interactions of fully hydrated dioleoylphosphatidylcholine bilayers. *Biophys. J.* 75:917–925.

40. Tironi, I. G., R. Sperb, P. E. Smith, and W. F. van Gunsteren. 1995. A generalized reaction field method for molecular dynamics simulations. *J. Chem. Phys.* 102:5451–5459.

41. Ziegler, A., X. L. Blatter, A. Seelig, and J. Seelig. 2003. Protein transduction domains of HIV-1 and SIV TAT interact with charged lipid vesicles. Binding mechanism and thermodynamic analysis. *Biochemistry.* 42:9185–9194.

42. Ziegler, A., P. Nervi, M. Dürrenberger, and J. Seelig. 2005. The cationic cell-penetrating peptide CPP(TAT) derived from the HIV-1 protein TAT is rapidly transported into living fibroblasts: optical, biophysical, and metabolic evidence. *Biochemistry.* 44:138–148.

43. Lin, J. H., and A. Baumgaertner. 2000. Stability of a melittin pore in a lipid bilayer: a molecular dynamics study. *Biophys. J.* 78:1714–1724.

44. Herce, H. D., A. E. Garcia, and T. Darden. 2007. The electrostatic surface term: (I) periodic systems. *J. Chem. Phys.* 126:124106.

45. Vives, E. 2005. Present and future of cell-penetrating peptide mediated delivery systems: ''Is the Trojan horse too wild to go only to Troy?'' *J. Control. Release.* 109:77–85.

46. Magzoub, M., and A. Gräslund. 2004. Cell-penetrating peptides: small from inception to application. *Q. Rev. Biophys.* 37:147–195.

47. Marrink, S. J., A. H. de Vries, and A. E. Mark. 2004. Coarse grained model for semiquantitative lipid simulations. *J. Chem. Phys.* 108: 750–760.

48. Tieleman, D. P., and S. J. Marrink. 2006. Lipids out of equilibrium: energetics of desorption and pore mediated flip-flop. *J. Am. Chem. Soc.* 128:12462–12467.

49. Babakhani, A., A. A. Gorfe, J. E. Kim, and J. A. McCammon. 2009. Thermodynamics of peptide insertion and aggregation in a lipid bilayer. *J. Phys. Chem. B.* 112:10528–10534.